have been recognized as critical elements in metastatic tumor growth and vascularization. Also the high interstitial fluid pressure (IFP) in tumor is a barrier for efficient drug delivery which lowers the therapeutic efficiency[Heldin, Rubin and Pietras, et al. (2004)].

The experiment research showed that the primary tumor in the Lewis lung model system was capable of generating a factor which was named angiostatin later suppressing the neovascularization and expansion of tumor metastases [O'Reilly, Holmgren and Shing, et al. (1994)]. Angiostatin is a 38-kD internal peptide of plasminogen, which is a potent inhibitor of angiogenesis in vivo, and selectively inhibits endothelial cell (EC) proliferation and migration in vitro. Tumor cells express enzymatic activity which is capable of hydrolyzing plasminogen to generate angiostain[Sim, O'Reilly and Liang, et al. (1997)]. Angiostatin is then transported and accumulated in the blood circulation in excess of the stimulators and thus inhibit angiogenesis of a metastatic tumor. A schematic diagram of this process is given in Fig.1. Angiostatin, by virtue of its longer half-life in the circulation [Paweletz and Knierim (1989)], reaches the vascular bed of metastatic tumor. As a result, growth of a metastasis is restricted by preventing and inhibiting of angiogenesis within the vascular bed of the metastasis itself.

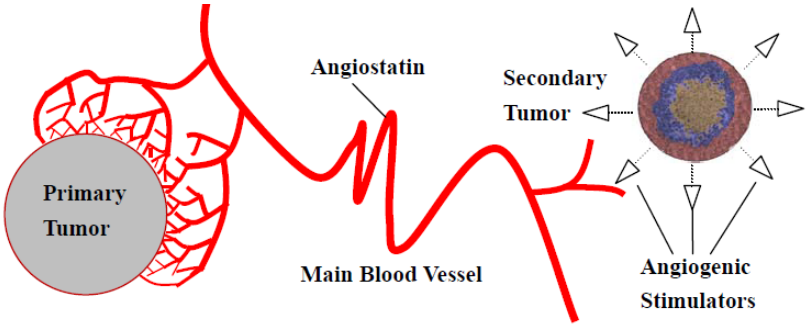


**Figure 1:** Schematic representation of angiostatin is transported from a fully vascularised primary tumor to its relation to a distant secondary tumor.

Although there are a number of mathematical models of metastatic tumors, there appears to be little in the literature by way of mathematical modelling of the mechanisms of anti-angiogenic activity of angiostatin on blood flow and interstitial fluid pressure in a metastatic tumor. Liotta et al[Liotta, Kleinerman and Saidel (1974)] first developed an experimental model to quantify some of the major processes initiated by tumor transplantation and culminating in pulmonary metastases. The study suggested that 'dynamics of hematogenously initiated metastases depended strongly on the entry rate of tumor cell clumps into the circulation, which in turn was intimately linked to tumor vascularization'. Later in the study Liotta et al[Liotta, Kleinerman and Saidel (1974)] confirmed his former observation and raised the idea that 'larger clumps produce significantly more metastatic foci than do smaller clumps matched for the number of cells'. Saidel et al[Saidel, Liotta and Kleinerman (1976)]proposed a lumped-parameter, deterministic model of the haematogenous metastatic process from a solid tumor, which provided a general theoretical framework for analysis and simulation. Numerical solutions of the model were in good agreement with their experimental results [Liotta, Kleinerman and Saidel (1974)]. The possibilities of anti-invasion and anti-metastatic

strategies in cancer treatment have bestowed an added preponderance with the keen interest in the mathematical modelling in the areas of tumor invasion and metastasis. Orme and Chaplain [Orme and Chaplain (1996)] presented a simple mathematical model of the vascularization and subsequent growth of a solid spherical tumor and gave a possible explanation for tumor metastasis, whereby tumor cells entered the blood system and secondary tumor may rise with the transportation function of blood. Sleeman and Nimmo [Sleeman and Nimmo (1998)] modified the model of fluid transport in vascularized tumors by Jain and Baxter [Baxter and Jain (1989)] to take tumor invasion and metastasis into consideration. Although these models did provide some features of tumor metastasis and interstitial fluid transportation such as perturbation analysis, they lacked in providing more detail information of metastatic tumor and as such were of limited predicted value. More realistic models of metastasis and interstitial fluid transportationwere developed to better understand its mechanism. Anderson et al [Anderson, Chaplain and Newman et al. (2000),] presented a discrete model from the partial differential equations of the continuum models which implied that haptotaxis was important for tumor metastasis. Iwata et al [Iwata, Kawasaki and Shigesada (2000)] proposed a partial differential equation (PDE) that described the metastatic evolution of an untreated tumor and its predicted results agreed well with successive data of a clinically observed metastatic tumor. Benzekry et al [Benzekry, Gandolfi and Hahnfeldt (2014)] proposed an organism-scale model for the development of a population of secondary tumors that takes into account systemic inhibiting interactions among tumors due to the release of a circulating angiogenesis inhibitor. Baratchart et al [Baratchart, Benzekry and Bikfalvi, et al. (2015)] derived a mathematical model of spatial tumor growth compared with experimental data and suggested that the dynamics of metastasis relied on spatial interactions between metastatic lesions. Stephanou et al [Stéphanou, Mcdougall and Anderson, et al. (2005)] investigated chemotherapy treatment efficiency by performing a Newtonian fluid flow simulation based on a study of vascular networks generated from a mathematical model of tumor angiogenesis. Wu et al [Wu, Long and Xu, et al. (2009)] extended the mathematical model into a 3D case to investigate tumor blood perfusion and interstitial fluid movements originating from tumor-induced angiogenesis. Soltani et al [Soltani and Chen (2013)] first studied the fluid flow in a tumor-induced capillary network and the interstitial fluid flow in normal and tumor tissues. The model provided a more realistic prediction of interstitial fluid flow pattern in solid tumor than the previous models. Some related works have been done on tumor induced angiogenesis, blood perfusion and interstitial fluid flow in the tumor microenvironment by using 2D mathematical methods[Zhao, Yan and Chen, et al.(2013); Wu, Ding and Cai, et al. (2011); Cai, Wu and Gulnar, et al. (2009); Jain, Tong and Munn (2007)] .In spite of the valuable body of work performed in simulation of blood perfusion, interstitial fluid flow and metastasis, previous studies have not examined blood perfusion and interstitial fluid pressure in the metastatic tumor microcirculation based on the microvascular network response to inhibitory effect of angiostatin which plays a significant role in suppressing tumor growth and metastasis.

Metastatic tumor blood perfusion and interstitial fluid transport based on 3D microvasculature response to inhibitory effect of angiostatin are investigated in this paper for exploring the suppression of metastatic tumor growth by the primary tumor. The abnormal geometric and

morphological features of 3D microvasculature network inside and outside the metastatic tumor, and relative complex and heterogeneous hemodynamic characteristics in the presence and absence of angiostatin can be studied in the 3D case. The simulation results may provide beneficial information and theoretical basis for clinical research on anti-angiogenic therapy.

## 2 Mathematical models

### *2.1 metastatic tumor angiogenesis*

3D mathematical model we present in this section originates from the previous 2D tumor anti-angiogenesis mathematical model [Zhao, Yan and Chen, et al.(2013); Jain, Tong and Munn (2007)] describing how capillary networks form in a metastatic tumor in response to angiostatin released by a primary tumor. The conservation equation of endothelial cells (EC) indicates the migration of EC influenced mainly by four factors: random motility, inhibitory effect of angiostatin, chemotaxis and haptotaxis. By using the seven-point finite difference scheme, we get the discretized equations which simulate the growth of capillary at every time step. The generated microvascular network inside and outside the metastatic tumor in the presence of angiostatin and in the absence of angiostatin are shown on Fig.2. General morphological features of the network such as growth speed, capillary number, vessel branching order and anastomosis density in/outside the metastatic tumor are consistent with the physiological observed results which indicates that angiostatin secreted by the primary tumor dose have an inhibitory effect on metastatic tumor[Orme and Chaplain (1996); Jain, Tong and Munn (2007)].

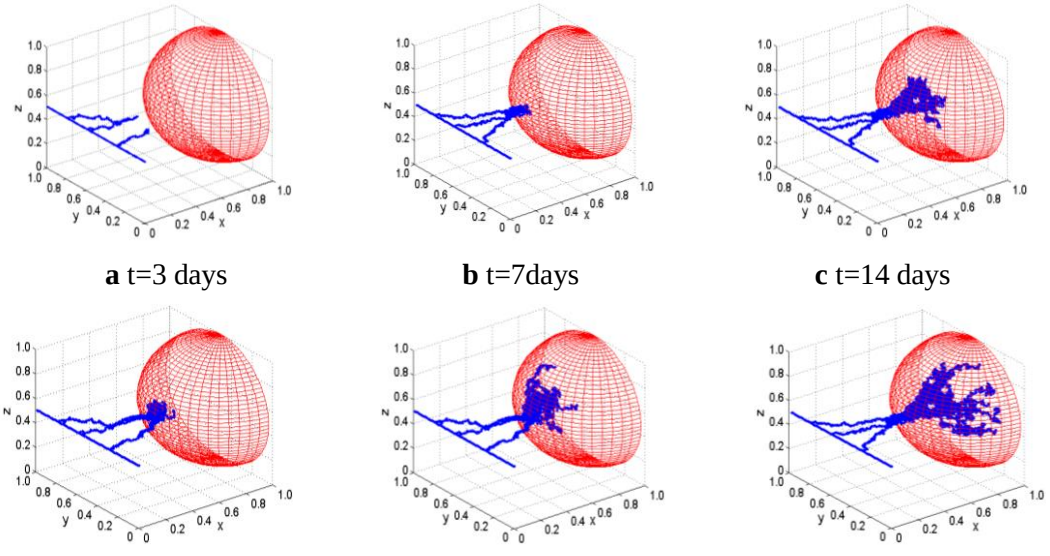

**a** t=3 days **b** t=7days **c** t=14 days

**d** t=3 days **e** t=7days **f** t=14 days

**Figure 2:** The spatio-temporal dynamic growth of 3D microvascular networks inside and outside the metastatic tumor. **a-c**) in the presence of angiostatin **d-f**) in the absence of angiostatin.

### *2.2 Blood perfusion*

To calculate flow through a given 3D microvascular network of interconnected capillary elements, assuming flux conservation and incompressible flow at each junction where the capillary elements meet

$$\sum_{n=1}^{6} Q^{n}_{(l,m,j)} \cdot B^{n}_{(l.m,j)} = 0 \tag{1}$$

where $B^{n}_{(l,m,j)}$ takes the integer 1 or 0, representing the connectivity between node $(l,m,j)$ and its adjacent node $n$. $Q^{n}_{(l,m,j)}$ is the flow rate from node $(l,m,j)$ to node $n$ and is given by $Q^{n}_{(l,m,j)} = Q^{n}_{v,(l,m,j)} - Q^{n}_{t,(l,m,j)}$, where $Q^{n}_{v,(l,m,j)}$ is the vascular flow rate without fluid leakage, described locally by Poiseuille's law

$$Q^{n}_{v,(l.m,j)} = \frac{\pi R_n^4 \left( p_{v,(l,m,j)} - p_{v,(n)} \right)}{8\mu_n \Delta L_n} \tag{2}$$

and $Q^{n}_{t,(l,m,j)}$ is the transvascular flow rate, following Starling's law

$$Q^{n}_{t,(l,m,j)} = 2\pi R_n \Delta \mathrm{L}_n \cdot L_{pv} \left[ \left( \bar{p}^{n}_{v,(l,m,j)} - \bar{p}^{n}_{i,(l,m,j)} \right) - \sigma_t \left( \pi_v - \pi_i \right) \right] \tag{3}$$

where $p_{v,(l,m,j)}$ and $p_{v,(n)}$ are the intravascular pressure of node $(l,m,j)$ and node $n$; $\bar{p}^{n}_{v,(l,m,j)}$ is the mean pressure in vascular element $(l,m,j)$; $\bar{p}^{n}_{i,(l,m,j)}$ is the mean interstitial pressure outside of vascular element $(l,m,j)$. $\mu_n$, $R_n$ and $\Delta L_n$ are the blood viscosity, radius and length of the vessel element $n$, respectively; $L_{pv}$ is the hydraulic permeability of vascular wall; $\sigma_t$ is the average osmotic reflection coefficient for plasma proteins; $\pi_v$ and $\pi_i$ are the colloid osmotic pressure of plasma and interstitial fluid.

### *2.3 Interstitial flow in metastatic tumor*

Considering the metastatic tumor tissue as an isotropic porous medium, its interstitial flow is modeled by Darcy's law [Baxter and Jain (1990)]

$$\boldsymbol{u}_i = -\kappa \nabla p_i \tag{4}$$

where $\boldsymbol{u}_i$ is the interstitial fluid velocity; $\kappa$ is the hydraulic conductivity coefficient of the interstitium; $p_i$ is the interstitial pressure.

The continuity equation is given by

$$\nabla \cdot \boldsymbol{u}_i = \phi_b \tag{5}$$

where $\phi_b$ is the fluid source term to couple the intravascular flow with the interstitial flow, which is heterogeneously distributed in the interstitial space and described by Starling's

law $\phi_b = \frac{L_{pv} S}{V}\left(p_v - p_i - \sigma_t\left(\pi_v - \pi_i\right)\right)$. where $S/V$ is the surface area per unit volume for transport in the interstitium.

Mass conservation at each junction where the interstitial fluid pressure satisfies equation

$$\nabla^2 p_i = \frac{\alpha^2}{R^2}\left(p_i - p_e\right)\cdot B \tag{6}$$

where $p_e = p_v - \sigma_t\left(\pi_v - \pi_i\right)$ is the effective pressure and $\alpha = R\sqrt{L_{pv} S/\kappa V}$ is the ratio of interstitial to vascular resistances to fluid flow. The continuity of pressure and flux on the interconnected boundary between the tumor and normal tissue $\Gamma$ : $p_i\big|_{\Gamma^-} = p_i\big|_{\Gamma^+}$, $-\kappa_T \nabla p_i\big|_{\Gamma^-} = -\kappa_N \nabla p_i\big|_{\Gamma^+}$, $\kappa_T$ and $\kappa_N$ are the hydraulic conductivity coefficients of normal tissue and tumor tissue, respectively.

Table 1 shows the values of the parameters used in the microcirculation simulations.

**Table 1:** Baseline parameter values used in the simulations.

| Parameter | Value | Parameter | Value |
|---|---|---|---|
| $\sigma_t^a$ | $8.7\times10^{-5}{}_{\mathrm{T}}$<br>$0.91_{\mathrm{N}}$ | $\left(\frac{S_v}{V}\right)^a$ | $50_{\mathrm{T}}\,\mathrm{cm}^{-1}$<br>$50_{\mathrm{N}}\,\mathrm{cm}^{-1}$ |
| $\pi_v{}^a$ | $19.8_{\mathrm{T}}\,\mathrm{mmHg}$<br>$20_{\mathrm{N}}\,\mathrm{mmHg}$ | $\pi_i{}^a$ | $17.3_{\mathrm{T}}\,\mathrm{mmHg}$<br>$10_{\mathrm{N}}\,\mathrm{mmHg}$ |
| $p_L{}^c$ | $0.5_{\mathrm{N}}\,\mathrm{mmHg}$ | $\frac{L_{pL} S_L}{V}{}^c$ | $0_{\mathrm{T}}\ 1/\mathrm{mmHg}\cdot\mathrm{s}$<br>$1.0\times10^{-4}{}_{\mathrm{N}}\ 1/\mathrm{mmHg}\cdot\mathrm{s}$ |
| $\kappa^a$ | $2.5\times10^{-7}{}_{\mathrm{T}}\,\mathrm{cm}^2/\mathrm{mmHg}\cdot\mathrm{s}$<br>$2.5\times10^{-7}{}_{\mathrm{N}}\,\mathrm{cm}^2/\mathrm{mmHg}\cdot\mathrm{s}$ | $L_{pv}^a$ | $1.86\times10^{-6}{}_{\mathrm{T}}\,\mathrm{cm/mmHg}\cdot\mathrm{s}$<br>$3.6\times10^{-8}{}_{\mathrm{N}}\,\mathrm{cm/mmHg}\cdot\mathrm{s}$ |
| $\mu^b$ | 1.0cP | | |

[a] Jain et al.[Jain, Tong and Munn (2007)][b] Stephanou et al[Stéphanou, Mcdougall and Anderson et al. (2005)]. [c]Zhao et al. [Zhao, Wu and Xu et al. (2007)]. Subscript 'N' and 'T' represents the values in normal and tumor tissues, respectively.

## 3 Simulation results

### *3.1 Blood perfusion of metastatic tumor*

We simulated the evolution of blood flow pressure with or without angiostatin for 14 days representing the typical timescale for tumor vasculature to grow. Fig.3 shows the

snapshots of the pressure profiles of blood flow through each vessel segment in a three-dimensional microvascular networks. We keep the inlet pressure and outlet pressure across parent vessel fixed at 25mmHg and 16mmHg[Zhao, Wu and Xu, et al. (2007)] in the simulation, in accordance with physiological values at the capillary scale. Fig.3 highlights a direct comparison of blood pressure distributions (Fig.3.a-c shows the blood pressure distribution with angiostatin, Fig.3.d-f shows the blood pressure distribution without angiostatin). We observe that the overall blood pressure is higher in the presence of angiostatin than that in the absence of angiostatin over the same growth duration. The blood flow distribution is complex and chaotic which makes the variety of blood pressure is small in the interior of the metastatic tumor compared to its exterior, contributing to the difficulties of efficient drug delivery in metastatic tumor. In the presence of angiostatin, the pressure-flows within some of the daughter vessels are elevated from the branching points to the metastatic tumor surface which provides effective blood perfusion and thus efficient therapeutic agents to the tumor. The simulation results indicate that blood perfusion varies significantly with the complex and chaotic three-dimensional microvascular networks inside and outside the metastatic tumor. The poor blood perfusion can be improved through the increased intravascular pressure with the presence of angiostatin. These results suggest that the inhibitory effect of angiostatin can affect the distribution of blood flow pressure and improve drug delivery to tumor.

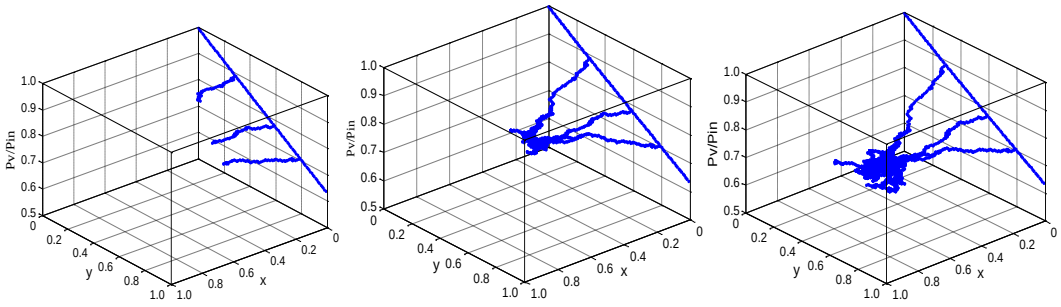


**a** t=3 days **b** t=7days **c** t=14 days

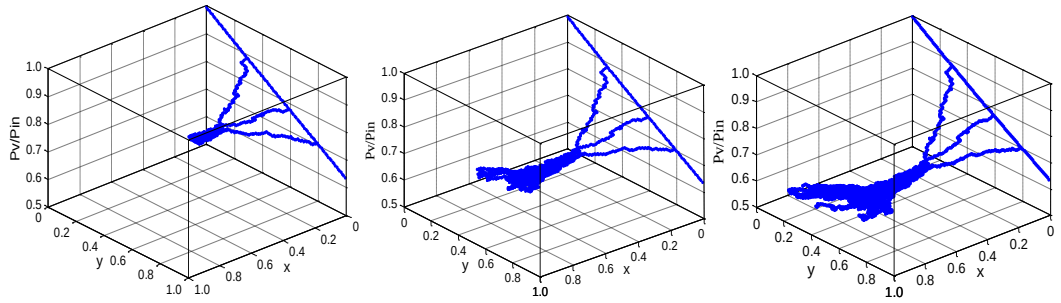


**d** t=3 days **e** t=7days **f** t=14 days

**Figure 3:** Simulations of blood pressure through 3D microvascular networks over time.a-c) Example simulation with angiostatin. d-f) Example simulation without angiostatin. Simulation domain is $[0,1]\times[0,1]\times[0,1]$. Blood enters the networks at the end of the parent vessel $(x=0, y=0, z=0.5)$, distributes throughout the capillary network,leaves from the end of the parent vessel $(x=0, y=1, z=0.5)$

### *3.2 Interstitial fluid flow of metastatic tumor*

Fig.4 shows the distribution of interstitial fluid pressure (IFP) within the metastatic tumor under the two mentioned situations. From the simulation results, we obtain that maximum IFP near the tumor center significantly dropped from 3.3, 11.48 and 11.53 mmHg to 0, 4.7 and 10.3mmHg with the presence of angiostatin at t=3,7 and 14 days, respectively, which indicated the IFP plateau is well relieved. As the growth days increase, IFP gradually elevate throughout the 3D metastatic tumor and the high pressure zone is at the center of the tumor and diminishes to the periphery and later becomes flatter. Comparing Fig.4.a-c to Fig.4.d-f, we come to conclude that angiostatin decrease the high IFP in the tumor, thus with the lower tarnsvascular pressure in the 3D heterogeneous capillary networks, leading to an significantly improved situation for interstitial convection which plays a significant role in non-uniform distribution of drug delivery to the metastatic tumor. These results provide important references for cancer prevention and treatment. Furthermore, anti-angiogenic therapies can normalize tumor vasculature and microenvironment, at least transiently in both preclinical and clinical settings[Jain, Tong and Munn (2007)].

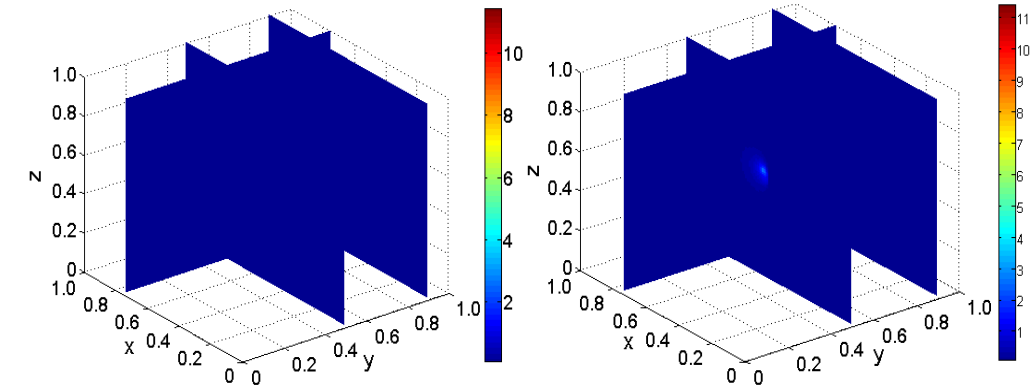


**a** t=3 days




**d** t=3 days

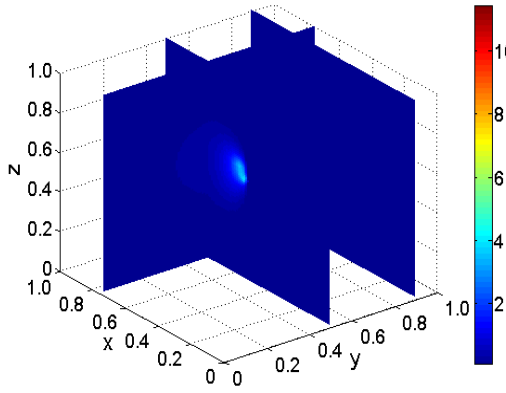


**b** t=7days

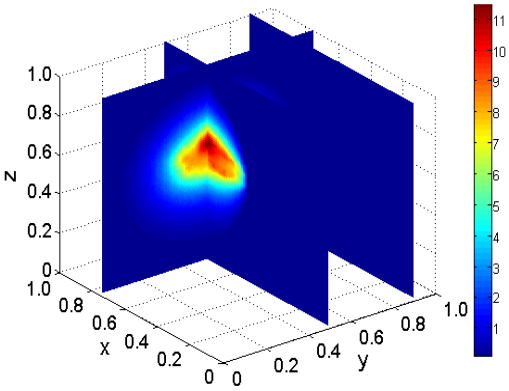


**e** t=7days

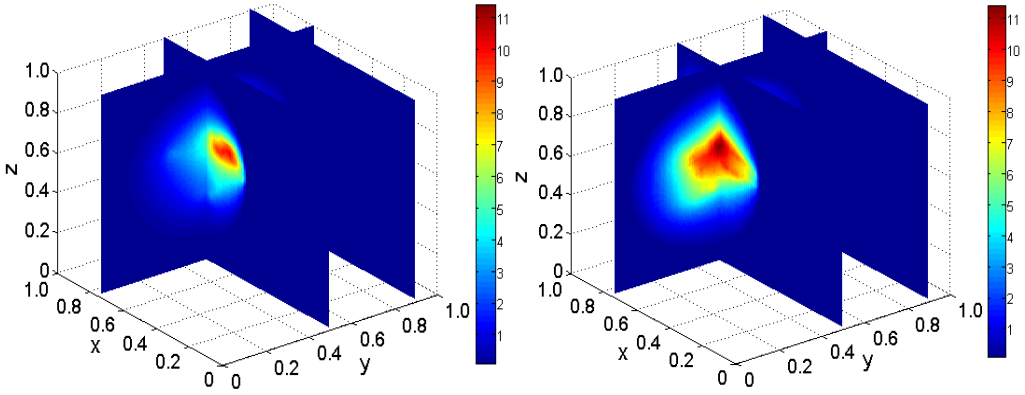


**c** t=14 days **f**t=14 days

**Figure 4:** Interstitial fluid pressure distributions within the metastatic tumor: **a-c)** in the presence of angiostatin; **d-f)** in the absence of angiostatin on the same other conditions

## 4 Conclusion

The inhibitory effect of angiostatin on the growth of metastatic tumor has been observed in some clinical and experimental malignancies. In this paper, we develop three-dimensional mathematical models describing the metastatic tumor microvasculature and microenvironment to investigate the inhibitory effect of anti-angiogenic factor angiostatin secreted by the primary tumor on metastatic tumor angiogenesis, blood perfusion, and interstitial fluid flow. Simulation results demonstrate that angiostatin has an obvious impact on the morphology, expansion speed, capillary number, vessel branching order inside and outside the metastatic tumor. 2D and 3D mathematical models of tumor anti-angiogenesis predict similar morphological behavior, such as vessels' length, branching patterns, anastomosis density or geometric distribution, for metastatic tumor angiogenesis under the inhibitory efficiency of angiostatin. However, capillary number and microvascular density due to space growth of vessel networks are increased in the 3D model. Furthermore, the simulations reflect the influences of heterogeneous blood perfusion, widespread interstitial hypertension, and low convection within the 3D metastatic tumor by carrying out a comparative study relating to the inhibitory effect of angiostatin. We find that 2D anti-angiogenesis model may be well suited to studying morphological behavior of vessel networks in the metastatic tumor, but 3D anti-angiogenesis model can better analyze blood perfusion, interstitial fluid flow, or oxygen and nutrient transport within the metastatic tumor microenvironment based on its more realistic 3D microvascular networks. Although 3D simulation results are consistent with the experimental observed facts and can provide more detailed space-information, however, angiogenesis and hemodynamics in the metastatic tumor by the anti-angiogenic therapy are very complex. To further research tumor angiogenic mechanisms and help to improve anti-angiogenic cancer therapy, more realistic features and complex biology factors need to be incorporated within the 3D model, such as the anatomy and physiology

of the metastatic tumor, drug delivery of anti-angiogenic therapy, behaviors of cells adhesion and interaction and the coupled with the various factors or other therapies strategies.

**Acknowledgments**: This work is supported by the National Natural Science Foundation of China (Grant Nos. 11502146, 51106099 and11572200), Shanghai Natural Science Foundation (No. 15ZR1429600).

**References**

**Anderson, A. R. A.; Chaplain, M. A. J.; Newman, E. L.; Steele, R. J. C.; Thompson, A. M.** (2000): Mathematical Modeling of Tumour Invasion and Metastasis. *Journal of Theoretical Medicine*, vol. 2, pp. 129-154.

**Baratchart, E.; Benzekry, S.; Bikfalvi, A.; Colin, T.; Cooley, L. S.; Pineau, R.; Ribot, E. J.; Saut, O.; Souleyreau, W.**(2015): Computational modelling of metastasis development in renal cell carcinoma. *Plos computational biology*, vol. 11, pp. e1004626.

**Baxter, L. T.; Jain, R. K.** (1989): Transport of fluid and macromolecules in tumors. I. Role of interstitial pressure and convection. *Microvascular Research*, vol. 37, pp. 77-104.

**Baxter, L.T.; Jain, R. K.**(1990): Transport of fluid and macromolecules in tumors.II. Role of heterogeneous perfusion and lymphatics. *Microvas. Res*, vol. 40, pp.246–263.

**Benzekry, S.; Gandolfi, A.; Hahnfeldt, P.**(2014): Global dormancy of metastases due to systemic inhibition of angiogenesis. *Plos One*, vol. 9, pp. e84249.

**Cai, Y.; Wu, J.; Gulnar, K.; Zhang, H.; Cao, J.; Xu, S.; Long, Q.; Collins, M. W.** (2009): Numerical simulation of solid tumor angiogenesis with Endostatin treatment: a combined analysis of inhibiting effect of anti-angiogenic factor and micro mechanical environment of extracellular matrix. *Appl.Math. Mech*, vol. 30, pp. 1247–1254.

**Folkman, J.** (1971): Tumor angiogenesis: therapeutic implications. *New England Journal of Medicine*, vol. 285, pp.1182-1186.

**Heldin, C. H.; Rubin, K.; Pietras, K.; Ostman, A.** (2004): High interstitial fluid pressure an obstacle in cancer therapy. *Nature Reviews Cancer*, vol. 4, pp. 806-813.

**Iwata, K.; Kawasaki, K.; Shigesada, N.** (2000): A dynamical model for the growth and size distribution of multiple metastatic tumors. *Journal of theoretical biology*, vol.203, pp. 177-186.

**Jain, R. K.; Tong, R. T.; Munn, L. L.**(2007): Effect of Vascular Normalization by Antiangiogenic Therapy on Interstitial Hypertension, Peritumor Edema, and Lymphatic Metastasis: Insights from a Mathematical Model. *Cancer Research*, vol. 67, pp. 2729.

**Konjevi, G.; Stankovi, S.**(2006): Matrix metalloproteinases in the process of invasion and metastasis of breast cancer. *Arch. Oncol*, vol. 14, pp. 136–140.

**Lane, W. S.; Cao, Y. H.; Sage, E. H.; Folkman, J.**(1994): Angiostatin: a novel angiogenesis inhibitor that mediates the suppression of metastases by a Lewis lung carcinoma. *Cell*,vol. 79, pp. 315-328.

**Lapcevich, R.; Nancy C. A.**(1997): A recombinant human angiostatin protein inhibits

experimental primary and metastatic cancer. *Cancer Research*, vol. 57, pp. 1329.

**Liotta, L. A.; Kleinerman, J.; Saidel, G. M.** (1974): Quantitative relationships of intravascular tumor cells, tumor vessels, and pulmonary metastases following tumor implantation. *Cancer Research*, vol. 34, pp. 997.

**O'Reilly, M. S.; Holmgren, L.; Shing, Y.; Chen, C.; Rosenthal, R. A.; Moses. M.;**

**Sim, B. K.; O'Reilly, M. S.; Liang, H.; Fortier, A. H.; He, W.; Madsen, J. W.; Paweletz, N.; Knierim, M.**(1989): Tumor-related angiogenesis. *Critical Reviews in Oncology/hematology*. vol. 9, pp. 197-242.

**Orme, M. E.; Chaplain, M. A. J.**(1996): A mathematical model of vascular tumour growth and invasion. *Mathematical and Computer Modelling*, vol. 23, pp. 43-60.

**Saidel, G. M.; Liotta, L. A.; Kleinerman J.** (1976): System dynamics of a metastatic process from an implanted tumor. *Journal of Theoretical Biology*, vol. 56, pp. 417.

**Sleeman, B. D.; Nimmo, H. R.** (1998): Fluid transport in vascularized tumours and metastasis. *Ima Journal of Mathematics Applied in Medicine & Biology*, vol. 15, pp. 53.

**Soltani, M.; Chen, P.**(2013): Numerical Modeling of Interstitial Fluid Flow Coupled with Blood Flow through a Remodeled Solid Tumor Microvascular Network. *Plos One*, vol. 8, pp. e67025.

**Stéphanou, A.; Mcdougall, S. R.; Anderson, A. R. A.; Chaplain, M. A. J.** (2005): Mathematical modelling of flow in 2D and 3D vascular networks: *Applications to anti-angiogenic and chemotherapeutic drug strategies. Mathematical & Computer Modelling*, vol. 41, pp. 1137-1156.

**Wu, J.; Long, Q.; Xu, S.; Padhani, A. R.** (2009): Study of tumor blood perfusion and its variation due to vascular normalization by anti-angiogenic therapy based on 3D angiogenic microvasculature. *Journal of Biomechanics*, vol. 42, no.6, pp. 712-721.

**Zhao, G.; Wu, J.; Xu, S.; Collins, M. W.; Long, Q.; König, C. S.; Jiang, Y.; Wang, J.; Padhani, A. R.**(2007): Numerical simulation of blood flow and interstitial fluid pressure in solid tumor microcirculation based on tumor-induced angiogenesis. *Acta MechanicaSinica*, vol. 23, pp. 477-483.

**Zhao, G.; Yan, W.; Chen, E.; Yu, X.; Cai, W.**(2013): Numerical simulation of the inhibitory effect of angiostatin on metastatic tumor angiogenesis and microenvironment. *Bulletin of Mathematical Biology*,vol. 75, pp. 274-287.